

THE ADVANCED CAMERA FOR THE HUBBLE SPACE TELESCOPE

G.D. ILLINGWORTH

*UCO/Lick Observatory, University of California,
Santa Cruz, California 9506 USA*

H. FORD

*Department of Physics and Astronomy, Johns Hopkins University,
Baltimore, Maryland 21218 USA*

The Advanced Camera for Surveys (ACS) will increase HST's capability for surveys by a factor of ~ 10 . The ACS will have three cameras. The first, the Wide Field Camera (WFC), will be a high throughput (45% at 700 nm, including the HST optical telescope assembly (OTA)), wide field ($200'' \times 204''$), optical and I-band camera that is half critically sampled at 500 nm. The second, the High Resolution Camera (HRC), is critically sampled at 500 nm, and has a $26'' \times 29''$ field of view and 25% throughput at 600 nm. The HRC optical path will include a coronagraph which will improve the HST contrast near bright objects by a factor of ~ 10 . The third camera is a far ultraviolet, Solar-Blind Camera (SBC) that has a relatively high throughput (6% at 121.6 nm) over a $26'' \times 29''$ field of view.

1 Design Philosophy for the Advanced Camera

The ACS team is building an Advanced Camera for the Hubble Space Telescope which will have a high throughput, wide field, optical and I-band camera (WFC), a critically sampled high resolution camera (HRC), and a high throughput, moderate field of view far ultraviolet, solar-blind camera (SBC). See Ford et al. (1996) for a more complete discussion of the ACS. The Advanced Camera for Surveys (ACS) will increase HST's capability for surveys and discovery by at least a factor of ten. The key characteristics of the ACS are listed in Table 1. The WFPC2 (Wide Field Planetary Camera 2) characteristics are given for comparison; compared to the SBC, the FOC and COSTAR have full sampling, but a field of only $7'' \times 7''$ and throughput that is typically only $\sim 1.5\%$.

Our approach to the ACS design was driven by two facts. First, images obtained with the FOC/COSTAR and WFPC2 cameras demonstrate that HST can deliver superb spatial resolution. Second, HST imaging with the present cameras is seriously limited by low throughputs (FOC and WFPC2), small fields of view (FOC), and undersampling (WFPC2). These three factors work together to severely limit HST's utility for deep, high-resolution imaging and for deep surveys. The time required to survey an area of the sky to a given

Table 1: Key Characteristics of the Advanced Camera for Surveys

Prioritized Features	WFC		HRC		
	ACS WFC	WFPC2 f/12.9	ACS HRC	WFPC2 f/28.3	ACS SBC
Throughput incl. OTA (%)	45@700nm	14@600nm	25@600nm	14@600nm	6.1@121.6nm
at 800nm	36	6.6	14	6.6	6.1@121.6nm
at 400nm	34	5.3	20	5.3	5.3@130nm
at 200nm	—	0.012	12	1.2	4.1@140nm
					2.9@150nm
					1.7@160nm
Equiv. FOV	200" × 204"	143" × 143"	26" × 29"	35" × 35"	26" × 29"
Sampling (500nm)	Half	Quarter	Full	Half	Half*
Polarization	< 1%	~ 5%	< 5%	~ 5%	< 1%

*@295nm

limiting magnitude and a specified signal-to-noise ratio (SNR) is inversely proportional to product of the detector area and the net DQE when the SNR is limited by shot noise in the signal. When the SNR is limited by the shot noise in the background, the time is inversely proportional to $\text{Area} \times \text{DQE}^2$. The most conservative measure of HST's survey or discovery efficiency is thus $\text{Area} \times \text{DQE}$. We aim to improve HST survey efficiency in the optical, the far UV, and especially the I-band, by at least a factor of 10. To achieve this goal we are paying careful attention to: i) an optical design that minimizes the number of reflections, ii) high-reflectivity coatings on the mirrors, filters, and windows, and iii) obtaining CCDs with high quantum efficiency in the optical and the near IR for the WFC, and in the near UV and optical for the HRC.

The ACS must be built in approximately one-third the time and for one-quarter of the cost of the first and second generation HST instruments. Our primary strategy for building the ACS within the cost and schedule constraints set out in the NASA Announcement of Opportunity is reliance on the Space Telescope Imaging Spectrograph (STIS) design and technology. The SBC and HRC detectors and electronics are STIS design, and, in fact, for the SBC likely will be a STIS flight spare. The two 2K×4K WFC I-band detectors and electronics derive directly from STIS CCDs. Whenever possible, we use STIS electronics and STIS mechanisms. Approximately 70% of our electronics modules and mechanisms are "build to print" from STIS drawings. The ACS flight software derives from STIS and NICMOS software whenever possible.

The second aspect of cost control is a strongly integrated team consisting of the Johns Hopkins University and the ACS Science Team, the Goddard

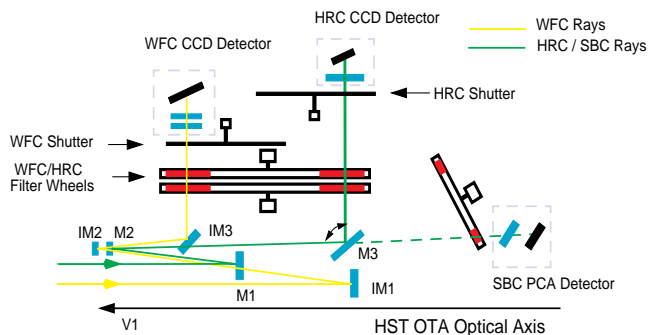


Figure 1: An optical schematic of the Advanced Camera

Space Flight Center, and Ball Aerospace. This ACS team minimizes management costs and maximizes scientific, managerial, and engineering resources which can be applied to building the ACS. The team members are Holland Ford (PI), Frank Bartko, Pierre Bely, Tom Broadhurst, Robert Brown, Chris Burrows, Edward Cheng, Mark Clampin, Jim Crocker, Paul Feldman, David Golimowski, George Hartig, Garth Illingworth, Randy Kimble, Carolyn Krebs, Tom La Jeunesse, Michael Lesser, George Miley, Susan Neff, Marc Postman, Marc Rafal, Bill Sparks, Zlatan Tsvetanov, Rick White, and Bob Woodruff.

The final aspect of ACS cost control is the science team’s philosophy of “keep it simple.” We prioritize our science goals and balance technical decisions on cost and performance against our most important science goals. We are not trying to achieve the unrealistic goal of building an Advanced Camera that will do everything for everyone.

2 Instrument Design

2.1 Overview of the Advanced Camera

The optical layout of the ACS is shown in Figure 1. The WFC and HRC have separate optical paths and mirrors. The WFC mirrors are designated IM1, IM2, and IM3. The HRC mirrors are designated M1, M2, and M3. The light in each optical path first encounters a spherical mirror (IM1 or M1) which images the HST pupil onto the IM2 (M2) mirror. These mirrors are anamorphic aspheres which are figured with the inverse spherical aberration on the HST primary mirror, and thus correct the spherical aberration in the HST primary and the field dependent astigmatism of the HST at the center

of the ACS field of view. The light from the WFC IM2 mirror is reflected by a Schmidt-like plate (IM3) through the two filter wheels to the WFC CCDs. The Schmidt plate corrects astigmatism over the WFC field of view (FOV).

The HRC and the SBC use the same M1 and M2 mirrors. The MgF_2 overcoatings on these two aluminum-coated mirrors are optimized for maximum reflectivity at 121.6 nm. Because of reflection losses in the far UV, we chose to have only two reflections in the optical path to the SBC. A flat mirror M3 is inserted into the light path to direct the light through the two filter wheels to the HRC 1024² CCD. The MgF_2 coating on M3 is optimized for maximum reflectivity at wavelengths >200 nm.

2.2 The Wide Field Camera

The WFC features a $200'' \times 204''$ field of view optimized for sky-limited V and I-band imaging. The WFC employs two butted SITe 2048×4096 CCDs with 15 micron pixels, with a plate scale of $0.051''/\text{pixel}$ and near critical sampling in the I-band. The high red throughput of the WFC is achieved by a unique optical design employing only three mirrors with protected silver coatings, and the use of thinned, backside-illuminated CCDs with anti-reflection coatings optimized for red wavelengths. The reflectivity of three silver coated mirrors is 50% higher than three aluminum coated mirrors would be at 800 nm. The mirror coating, as well as the geometry, yield less than one percent polarization sensitivity. Overcoated silver mirrors maintain high reflectivity for several years with exposure to typical laboratory air quality and humidity.

Figure 2 shows expected net WFC and HRC net efficiencies (including HST OTA) compared to the WFPC2. We have specified that the quantum efficiency (QE) at 800 nm must be $\geq 59\%$, with a goal of 68%. The maximum peak throughput must be $\geq 74\%$ with a goal of 77%.

2.3 The High Resolution Camera

The HRC provides spectral coverage from 200–1000 nm with a $26'' \times 29''$ field of view. The detector is a 1024×1024 STIS-like CCD manufactured by SITe. This CCD will be optimized for high quantum efficiency in the near UV by Mike Lesser at the University of Arizona. Lesser's process uses a platinum flashgate (PPtF) and an AR coating optimized for the 200–300 nm bandpass. If Lesser's process is not perfected in time to meet the ACS schedule, we will use a SITe CCD with a new SITe ultraviolet anti-reflection coating. Figure 3 shows the QE expected from Lesser's process, the QE from the new SITe UV coating, and the QE of the STIS CCD. The net HRC plus HST OTA efficiency is shown in Figure 2.

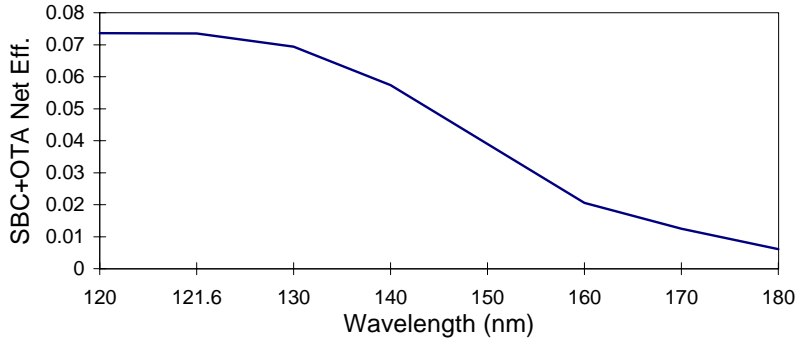


Figure 4: Expected SBC net efficiency (including the HST OTA) versus wavelength

The HRC image is critically sampled for wavelengths greater than 500 nm, with an average plate scale of $0.025''/\text{pixel}$. The HRC uses only two powered mirrors and a fold mirror to relay the HST field image to the CCD for highest throughput and lowest scatter. The HRC mirrors are coated with aluminum plus MgF_2 to achieve the highest possible reflectivity between 122 to 1000 nm.

2.4 The Solar Blind Camera

The SBC is optimized for highest throughput from 115 nm to 170 nm. The image is sampled at $0.030''/\text{pixel}$. The SBC uses a STIS-based PCA photon-counting detector with an opaque CsI photocathode and a C-plate micro-channel plate (MCP). The relay optics and corrector mirror mechanism are shared with the HRC camera. A full $26'' \times 29''$ FOV is available. The resultant image quality at the PCA MCP surface is better than $\lambda/8$ everywhere in the FUV, and nearly uniform with field. The design is optimized from 121.6 to 160.8 nm. The expected QE of the SBC detector, including the HST OTA, is shown in Figure 4.

3 Filters and Dispersers

We have simplified the optical design and reduced cost by sharing the filter wheels for the WFC and HRC, as well as sharing the corrector optical path for the HRC and SBC. The WFC and HRC filter wheel mechanism is comprised of two separate filter wheels, each driven by an independent motor and sharing a common housing. These filter wheels are populated with 17 bandpass filters (13 of which are spectrally compatible with both the WFC and HRC), a set of

five linear ramp filters, a grism for the WFC, and a prism and three visible and three ultraviolet polarizers for the HRC. The SBC has five longpass filters, two prisms, a narrow band Lyman- α filter, and four opaque positions. Altogether the ACS incorporates a total of 38 spectral elements. The large WFC filters can be used with the HRC. Figure 5 shows the bandpasses of the filters. Five of the broadband filters are based on the Sloan Digital Sky Survey filter set (g, r, i, z, and a modified u called wfcu).

Narrow-band filters for the WFC and HRC take three forms: standard narrow-band filters which cover the whole field of view of both cameras, linear ramp filters similar in concept to those on WFPC2, and an HRC methane band filter for observations of the giant planets. The standard narrow-band filter complement is H α , [O III] and [Ne V]. The four narrow-band ($\sim 2\%$) and one broadband ($\sim 9\%$) linear ramp filters provide an imaging capability for redshifted emission line sources. The desired bandpass is selected by a combination of target positioning and filter wheel rotation. The central strip of each of the five linear ramp filters can be used with the HRC.

Two sets of polarizers, one for the UV and the other for the visible, also are included for imaging with the HRC. Each set of polarizers consists of three separate elements to give relative polarizing angles of 0, 60, and 120 degrees. The SBC filter wheel contains a set of short-cut filters which step across the SBC bandpass. The broadest filter, MgF₂, transmits geocoronal Lyman- α , while the CaF₂ filter blocks geocoronal Lyman- α and transmits light longward of 125 nm. The ACS includes three prisms and a grism for deep, low spectral resolution imaging from 120 nm to 1000 nm (see Figure 5); the resolution of these is typically $R \sim 100$.

4 Coronagraph

The ACS coronagraph will have two high contrast options. Both options provide for suppression of the light from a bright object which is positioned behind a mask using autonomous on-board target acquisition. The first option is a "Fastie spot", which is a 0.8" diameter reflecting spot deposited near the corner of the HRC CCD entrance window (where the beam size is 0.5"). It will allow unvignetted high contrast imaging (including with the ramp filters) from 0.7" to 4" around a bright source (e.g., imaging of a quasar host galaxy.) Vignetted, but still useful data will be available all the way in to 0.4" from the source.

The second option is a commandable coronagraphic mask that can be positioned in the aberrated HST focal plane, together with a Lyot stop that is simultaneously positioned at the pupil image close to the M2 mirror. This

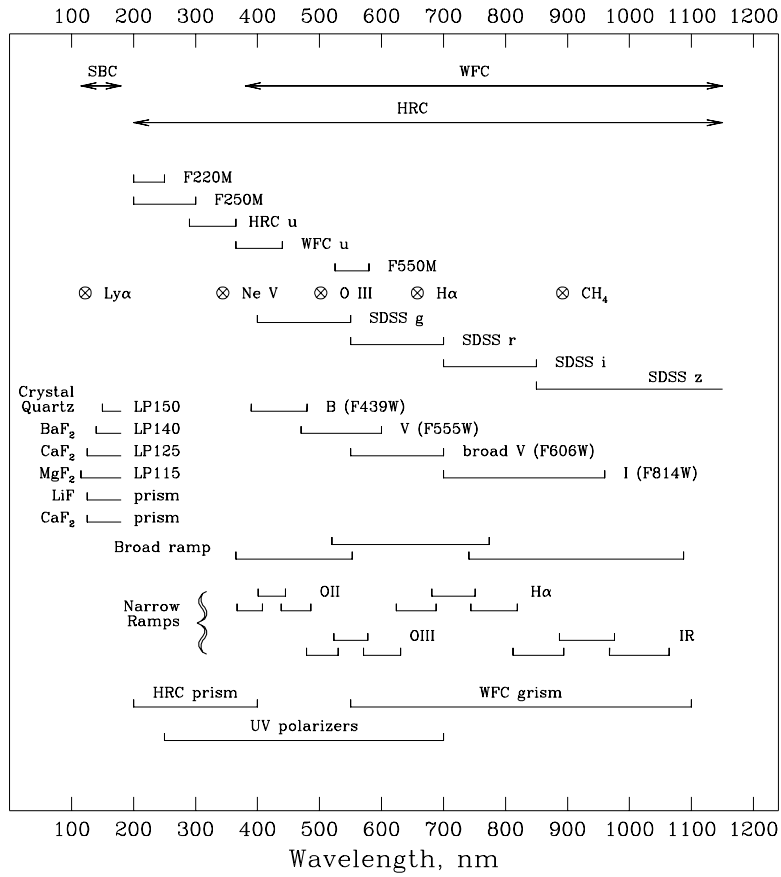


Figure 5: ACS filter summary ^aThe w

option does not interfere with normal camera operation in any way. The Lyot stop has the effect of removing the diffracted light halo that surrounds the target, giving almost an order of magnitude higher contrast improvement at the longest wavelengths. The residual halo that is present is caused by scatter from ripples in the primary and secondary mirrors.

5 Operational Modes

Two major operational features of the ACS improve its science productivity and provide efficient operation. The first feature allows the observer to simultaneously use two cameras for parallel imaging. This is made possible by two filter wheels (shared by the WFC and HRC for cost saving), containing a total of 30 filter positions, each of which can be used by the WFC and HRC, and a third 12-position filter wheel dedicated to the SBC.

The second feature allows simple WFPC2-like target acquisition because the fields of view of each camera are large compared to HST pointing uncertainties. Additionally, although each optical channel of the Advanced Camera is optimized for specific types of science, a number of operational features have been designed into the ACS to allow the observer to select permitted combinations of optical channels, to choose a particular readout mode, and to configure filter elements to enhance their specific science programs. For example, the large format and layout of the WFC CCD's make it particularly well suited for large-scale, deep mapping surveys, by making it possible to obtain contiguous exposures with single guide star acquisitions. The rows and columns of the WFC and HRC CCDs are parallel to the V2 and V3 axes, making it possible to efficiently "tile" a survey area while stepping the guide stars along the long directions of the FGS sensors.

Acknowledgments

The Advanced Camera is funded by NASA through the HST Project Office at the Goddard Space Flight Center.

References

Ford, H. et al. 1996, in *Space Telescopes and Instruments II*, SPIE Vol. 2807 (Bellingham, WA: SPIE), in press.